8072–8082 *Nucleic Acids Research, 2010, Vol. 38, No. 22*
doi:10.1093/nar/gkq755

Gene repression by minimal *lac* loops *in vivo*

Laura M. Bond[1], Justin P. Peters[1], Nicole A. Becker[1], Jason D. Kahn[2] and L. James Maher III[1,*]

[1]Department of Biochemistry and Molecular Biology, Mayo Clinic College of Medicine, 200 First St. SW, Rochester, MN 55905 and [2]Department of Chemistry and Biochemistry, University of Maryland, College Park, MD 20742-2021, USA

Received May 21, 2010; Revised and Accepted August 9, 2010

ABSTRACT

The inflexibility of double-stranded DNA with respect to bending and twisting is well established *in vitro*. Understanding apparent DNA physical properties *in vivo* is a greater challenge. Here, we exploit repression looping with components of the *Escherichia coli lac* operon to monitor DNA flexibility in living cells. We create a minimal system for testing the shortest possible DNA repression loops that contain an *E. coli* promoter, and compare the results to prior experiments. Our data reveal that loop-independent repression occurs for certain tight operator/promoter spacings. When only loop-dependent repression is considered, fits to a thermodynamic model show that DNA twisting limits looping *in vivo*, although the apparent DNA twist flexibility is 2- to 4-fold higher than *in vitro*. In contrast, length-dependent resistance to DNA bending is not observed in these experiments, even for the shortest loops constraining <0.4 persistence lengths of DNA. As observed previously for other looping configurations, loss of the nucleoid protein heat unstable (HU) markedly disables DNA looping *in vivo*. Length-independent DNA bending energy may reflect the activities of architectural proteins and the structure of the DNA topological domain. We suggest that the shortest loops are formed in apical loops rather than along the DNA plectonemic superhelix.

INTRODUCTION

The worm-like chain (WLC) polymer model accurately describes many important physical properties of the DNA polymer (1,2). According to the WLC model, a DNA molecule much longer than the polymer persistence (0.05 μm) is not rod-like. Such a molecule spontaneously collapses in solution to form a coil with the root mean squared end-to-end polymer distance equal to the square root of the product of contour length and persistence length. For example, the circular *Escherichia coli* genome contains 4.6 million base pairs (bp) of DNA with a contour length of 1600 μm. The WLC model predicts that the *E. coli* chromosome should coil to a volume of 200 μm^3 in solution. However, it is necessary to compact the chromosome an additional 400-fold to form the *E. coli* nucleoid, occupying only 0.5 μm^3 (a DNA concentration of ~50 mg/ml) within the rod-shaped bacterial cell. This additional compaction involves DNA supercoiling and wrapping about packaging proteins.

DNA stiffness has important biological implications (3). For example, tight wrapping of eukaryotic DNA onto histone octamers is energetically expensive. Favorable histone–DNA interactions must compensate for this cost. Because certain DNA sequences have bend/twist/stretch flexibility (4–6) or bonding interactions (7) that allow for preferred capture by histone octamers, DNA stiffness plays a central role in genome-wide histone-positioning codes in eukaryotes (8–10). Some restriction endonucleases require short-range DNA looping (11), as do prokaryotic recombination reactions. Because of intrinsic DNA stiffness, these processes are facilitated by sequence-non-specific DNA bending proteins, such as yeast Nhp6A or bacterial heat unstable (HU), which increase the apparent flexibility of DNA (12,13). Gene regulation in prokaryotes (14–18) and in yeast (19) can also involve DNA looping.

Classic (16,17,20–22) and more recent (23–28) experiments have employed components of the *E. coli lactose* operon as a model system to study DNA flexibility *in vitro* and *in vivo* (Figure 1A and B). Promoter repression by an operator just downstream of the *lac* promoter is enhanced by auxiliary operators further upstream or

*To whom correspondence should be addressed. Tel: +1 507 2849041, ext.: 98; Fax: +1 507 2842053; Email: maher@mayo.edu

The authors wish it to be known that, in their opinion, the first two authors should be regarded as joint First Authors.

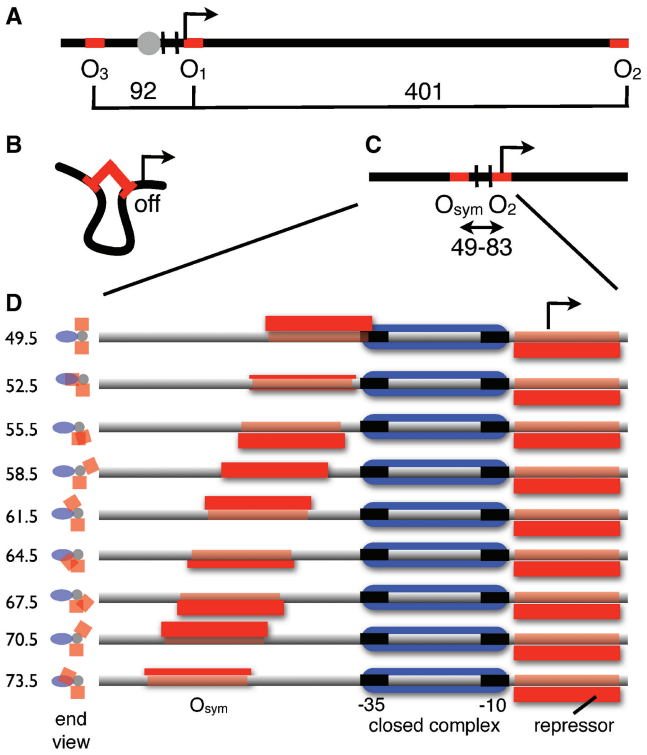

Figure 1. Experimental design. (**A**) Wild-type *E. coli lac* promoter indicating positions of transcription start point (broken arrow), −10 and −35 promoter elements (vertical lines), *lac* operators (red squares) and catabolite activator binding site (gray circle). (**B**) Schematic view of closed loop containing repressed promoter. Operators and tetrameric repressor are shown in red. (**C**) Experimental *lac* promoter designs to minimize DNA loop sizes for center-to-center operator spacings between 49 and 83 bp. (**D**) Enlargement of promoter region indicating predicted helical disposition of RNA polymerase closed complex (blue oval) and lac repressor proteins (red rectangles) for selected spacings along the DNA (gray). An end view (DNA observed from upstream) is displayed at left. The diagram is to scale based on 11 bp/turn as estimated from prior experiments.

downstream. The mechanism of enhanced repression has been shown to involve increased effective local concentration of bidentate lac repressor tetramers. These DNA-bound repressors collide with free operators by virtue of the intervening DNA tether, whose properties can then be studied by changing the tether length. Previous systematic studies of *in vivo* DNA looping with lac repressor have explored operator spacings (typically measured from operator center to operator center) of 127–197 bp (21), 58–100 bp (17) and 63–91 bp (23,26). Analysis of these results has invoked thermodynamic models (21,23,25,29) and mechanics calculations (30–34). Because repression looping requires close approach of the operators and is most stable when operators occur on the same DNA face (Figure 1B), reporter gene expression as a function of operator spacing yields information about both DNA bend and twist flexibility. Uncertainties about the physical properties and conformational flexibility of lac repressor tetramers limit quantitative estimates of DNA flexibility from such studies. However, DNA appears 2- to 7-fold softer to bending and twisting *in vivo* versus *in vitro* (21,31). Interestingly, DNA looping during recombination in eukaryotes has been measured *in vitro* and *in vivo*, also revealing chromatin flexibility to be higher than expected (35).

Our laboratory is interested in understanding these anomalies. We hypothesize that the presence of sequence-non-specific architectural proteins (36) may explain apparent DNA softness *in vivo*: transient protein-induced bending at random locations mimics increased bending flexibility. The *E. coli* HU protein has been shown to be important for repression looping in the *gal* (37–39) and *lac* (23–26) operons. Sequence-non-specific eukaryotic high-mobility Group B (HMGB) proteins can complement DNA looping in the absence of HU (12,13,23,25,26,40).

Studies of DNA flexibility *in vivo* are also relevant because of recent controversy concerning DNA-bending mechanisms (41–49). At issue has been whether the smooth bending implied by the WLC model is sufficient to describe DNA flexibility down to scales comparable with lac repression loops, or whether new bending regimes must invoke DNA kinking. A particularly interesting recent study (45) demonstrates that torsionally relaxed DNA is smoothly bent, without kinking even when the DNA is constrained into circles as small as 85 bp. This prompted us to design experiments to measure DNA looping *in vivo* for the smallest possible *lac* repression loops containing an *E. coli* promoter. Our goal was to determine if the DNA strain within *lac* repression loops is accommodated over short distances, where bending and twisting strain should be greatest. Our *in vivo* approach is conceptually similar to a classic *in vitro* study of DNA looping over ~50 bp by phage λ repressor (50).

Here, we show that plots of *in vivo lac* repression oscillate smoothly with *lac* operator spacing over the distances tested. We further show that these repression data can be easily misinterpreted at the smallest operator spacings. Control experiments reveal that close approach of a *lac* operator to the −35 promoter element causes loop-independent repression that must be considered. Accounting for this, we provide reporter gene expression data for *lac* repression loops at center-to-center *lac* operator spacings as short as 59.5 bp, the shortest distance where loop-independent repression is avoided. We further confirm that loss of the nucleoid protein HU strongly destabilizes DNA looping over these distances.

MATERIALS AND METHODS

Bacterial strains

FW102 (the kind gift of F. Whipple) is a Strep^R derivative of CSH142 [*araD*(*gpt-lac*)$_5$] and is designated as wild-type in this study. Strain BL463 carries chromosomal deletions in both *hupA* and *hupB* genes and is designated ΔHU (23). Gene deletions and the presence of looping assay episomes were confirmed by diagnostic PCR amplification following conjugation and selection.

DNA constructs

DNA looping constructs were based on plasmid pJ992, created by modifications of pFW11-null (51) as previously

described (23). Constructs contained a strong distal O_{sym} operator and a weak proximal O_2 operator. The design corresponds to Figure 5C in reference (25). Sequences of all experimental and control promoters are shown in Supplementary Figures S1 and S2 and Supplementary Tables S1 and S2. The O_2 operator normally present within the *lacZ*-coding region was destroyed by site-directed mutagenesis. A construct with a proximal O_2 but lacking upstream O_{sym} was used as a normalization control. Constructs lacking O_2 and with O_{sym} at various upstream positions were used as controls in some experiments. Test promoters do not contain promoter catabolite activator protein binding sites. *lacZ* looping constructs were placed on the single copy F128 episome by homologous recombination between the constructed plasmids and bacterial episome. F128 carries the *lacI* gene producing wild-type levels of repressor. Bacterial conjugation and selections were as previously described (51).

In vivo DNA looping assay and data fitting

Analysis of *lac* reporter gene expression was performed as described (25). Raw β-galactosidase reporter activity (E) is presented in Miller units. Normalized E'-values are then obtained by dividing E-values by E obtained for a test construct where specific looping is not possible because only a single proximal O_2 operator is present in the absence of an upstream O_{sym} operator. The repression ratio (RR) is given by $E_{induced}/E_{repressed}$, where induction is obtained by addition of 2 mM isopropyl β-D-1-thiogalactopyranoside (IPTG). Best fits to the thermodynamic model of *lac* gene regulation produced estimates of 12 parameters (set of six for repressed or induced) along with 95% confidence limits for error ranges. These parameters provide a description of the specifically (and non-specifically) looped, singly bound and free states of the O_2 operator under repressed and induced conditions. In this context, *hr* is the DNA helical repeat, C_{app} is the apparent torsional modulus of the DNA loop, $sp_{optimal}$ is the optimal spacing between operators (in bps) where *sp* is the actual spacing for a given construct, K_{max} is the equilibrium constant for the formation of a (specific) loop with perfect phasing, K_{NSL} is the equilibrium constant for non-specific looping, and P_{app} is an empirical parameter that captures any observed decrease in DNA-bending free energy as *sp* increases. Equilibrium constants K°_{max} and K°_{NSL} (Table 1) are normalized values obtained by dividing fitted values of K_{max} and K_{NSL} by K_{O_2}, the equilibrium constant for repression by an isolated O_2 operator in the absence of looping. The values of K_{O_2} are independently estimated under repressed and induced conditions for each experiment (Table 1). These values replace the previous K_{O_2} estimates of 1.0 and 0 under repressed and induced conditions, respectively. Differences in K_{O_2} between different strain genetic backgrounds presumably reflect differences in lac repressor concentration and DNA accessibility. As noted earlier, the relationship between P_{app} and a true *in vivo* DNA persistence length is complex (25). Fittings were performed in two steps, first a global nonlinear least-squares refinement to E (repressed and induced) followed by a

Table 1. Parameters (95% confidence interval) fit to a thermodynamic model of lac repressor looping

	hr (bp/turn)		C_{app} ($\times 10^{-19}$ erg cm)		K_{O_2}		K°_{max}		K°_{NSL}		$sp_{optimal}$ (bp)		P_{app} (bp)	
	−IPTG	+IPTG	−IPTG	+IPTG	−IPTG	+IPTG	−IPTG	+IPTG	−IPTG	+IPTG	−IPTG	+IPTG	−IPTG	+IPTG
WT[a]	11.5 ± 0.7	10.7 ± 1.0	0.79 ± 0.21	0.64 ± 0.21	2.4	0.13	64 ± 29	1.0 ± 0.5	*11 ± 23*	*0 ± 1.3*	78.3 ± 0.5	78.8 ± 0.9	*37 ± 173*	*185 ± 210*
WT[b]	11.4 ± 0.3	9.6 ± 0.1	1.06 ± 0.15	2.67 ± 0.71	4.9	0.61	50 ± 7	1.9 ± 1.2	3 ± 1	*0 ± 0.1*	79.5 ± 0.5	79.8 ± 0.3	*0 ± 52*	*0 ± 131*
WT[c]	11.1 ± 0.2	10.7 ± 0.7	0.97 ± 0.03	1.65 ± 1.14	4.9	0.61	62 ± 15	0.9 ± 0.6	*0 ± 1*	*0 ± 0.1*	79.2 ± 0.1	80.2 ± 1.0	*0 ± 71*	*0 ± 390*
ΔHU[a]	10.9 ± 1.2	9.5 ± 2.5	0.66 ± 0.20	0.32 ± 0.17	3.2	0.46	17 ± 13	*0.2 ± 0.7*	*2 ± 10*	*0 ± 0.5*	76.9 ± 0.8	78.3 ± 2.4	*33 ± 274*	*308 ± 957*
ΔHU[c]	11.3 ± 0.2	10.5 ± 2.5	1.10 ± 0.13	0.35 ± 0.13	10.8	0.71	14 ± 3	*0.1 ± 0.1*	*0 ± 1*	*0 ± 0.1*	78.5 ± 0.3	79.6 ± 1.5	*0 ± 68*	*382 ± 500*

Parameters not well determined by fitting are indicated in italics.
[a]Fits based on data reported by Becker *et al.* (23). WT, wild-type *E. coli* strain. ΔHU, *E. coli* strain with *hupA* and *hupB* gene disruptions.
[b]Fits based on current data set for all operator spacings.
[c]Fits based on current data set after eliminating data for spacings. <59.5 bp where loop-independent repression is observed.

global nonlinear least-squares refinement to E (repressed and induced) and RR simultaneously with K_{max}, K_{NSL} and P_{app} estimates held fixed from the first fitting routine. Values and ranges for hr, C_{app} and $sp_{optimal}$ are reported from this second fitting. R version 2.8.1 was used for all data analysis and fitting. All data are included in Supplementary Table S3.

Structural modeling

DNA supercoiling was modeled with a simple geometric picture for a plectonemic superhelix with circular arcs as end caps forming the apical loops. For a given DNA length L and helical repeat hr, we calculate the writhe Wr for a given superhelical density as L/hr*0.85 (assuming that 85% of the linking number deficit ΔLk appears as writhe). All of the writhe is assumed to manifest in a uniform plectonemic superhelix based on the model used by Boles *et al.* (52). The superhelix pitch angle α is taken to be 60°. The superhelix radius r for the images in Figure 6 was set at the low end of physically reasonable values, 17 Å. The length of the end caps is calculated as the difference between the length of DNA in the superhelix $(|Wr|-1)\pi r/\cos\alpha$ and the total length. Each end cap is assumed to be composed of a nearly planar $(360-2\alpha)^\circ$ arc and two straight segments that exit the superhelix at a $(90-\alpha)^\circ$ relative to the helix axis. The lengths of the straight segments and the radius of the arc are calculated from the length of the end cap assuming planarity and then refined iteratively to allow for the straight segments being in planes separated by $2r$. Matlab code is available on request.

RESULTS AND DISCUSSION

Experimental design to minimize *lac* repression loop size

The experimental design for this study is shown in Figure 1C. The components of the *lac* repression loop system were assembled in a series of simplified constructs designed to minimize repression loop size while maintaining an *E. coli lac* UV5 promoter within the loop. Both the normal downstream O_2 operator and the catabolite activator binding site are removed. A weak 21-bp O_2 proximal *lac* operator (repressor binding site) begins 1-bp downstream of the −10 box. The transcription start site is at the sixth bp of the O_2 operator. It was previously shown that this placement of O_2 adjacent to the promoter −10 element does not alter the function or periodicity of *lac* repression loops (25). A strong O_{sym} operator is placed various distances upstream of the −35 promoter element so that O_2–O_{sym} center-to-center distances ranged from 49 to 83 bp. Promoter sequences are shown in Supplementary Figures S1 and S2.

This experimental design deliberately minimizes repression loop lengths to explore repression patterns for the stiffest possible DNA segments. This design requires close apposition of genetic elements, as shown in Figure 1D. The illustration shows predicted helical dispositions of operators (red), promoter elements (black) and the RNA polymerase (blue) modeled as a closed complex with the promoter (53). The elements are drawn approximately to scale, and helical disposition is based on a helical repeat of 11 bp/turn as previously fitted to data obtained with similar constructs *in vivo* (23). This helical repeat could reflect the influence of supercoiling because sites of closest approach trace out a helical path on a plectoneme (54). Operators are predicted to occur on the same DNA face at spacings of ~55, 66 and 77 bp, with loop-mediated repression expected to be maximal at these spacings.

Full repression data set and analysis

Unedited experimental data for reporter gene repression as a function of operator spacing are shown in Figure 2. The upper panel shows the conventional RR, defined as the reporter gene activity in the presence of IPTG inducer divided by the activity in the absence of inducer. Peaks represent maximal repression loop stability. The previous result for O_2 positioned 8 bp further downstream is shown in gray. The two curves in the lower panel depict reporter activity in the presence or absence of IPTG inducer. Raw reporter activities are normalized to the activity of a reporter construct where looping is disabled by

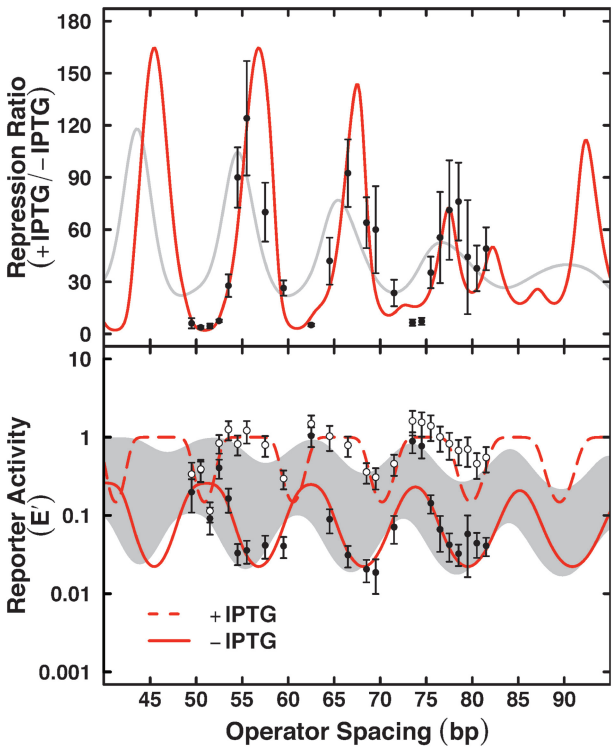

Figure 2. Reporter repression as a function of *lac* operator spacing using data for all spacing constructs studied here (transcription start site within downstream O_2). Upper panel shows RR, induced expression divided by repressed expression, closed circles, fitted to thermodynamic model shown by solid red line. Lower panel shows normalized reporter expression (E') in the presence (open circles) or absence (filled circles) of IPTG inducer. Fits to thermodynamic model are shown by red lines (25). Standard deviation is indicated. Also shown for comparison (gray line above, gray region below) are previous data for constructs with O_2 downstream from the transcription start point (23). Note the adequate fit to the thermodynamic model for the upper panel but not for the lower panel.

elimination of O_{sym}, to give the plotted E'-values (23,25). Also shown in Figure 2 are best fits to a thermodynamic model of *lac* gene regulation (23,25). Shown by gray shading is the region bounded by the corresponding fits for prior data from constructs with O_2 positioned 8 bp further downstream. The fitted parameter values for the unedited data set are given in Table 1.

Superficial examination of the repression data in Figure 2 show them to be consistent with prior results for larger DNA loops, with periodic dependence of repression on operator spacing continuing to the shortest separations tested (49.5 bp). This analysis tends to confirm previous reports (16,17,20,21,23–25), while extending measurements to shorter DNA loops than previously tested and demonstrating that optimal loop length does not depend on the precise position of the proximal operator. The data appear to show that DNA twisting strain remains the dominant obstacle to looping *in vivo*. Maximal repression values (troughs in E' data) are not appreciably dependent on DNA length over this range, suggesting that DNA bending energy is not affecting the rate-limiting step in transcription. Best fit parameters (Table 1) were comparable with those previously reported, with a fitted helical repeat >11 bp/turn consistent with the apposition of sites within a plectonemic superhelix. However, some data in Figure 2 (particularly E'-values) were not fit well by the thermodynamic model.

Evidence that protein–protein interactions complicate analysis of smallest repression loops

In fact, although the conventional RR data in Figure 2 depict a continuous periodic relationship between operator spacing and repression for constructs with operator spacings as short as 49.5 bp, further studies revealed a more complex picture. E'-values (normalized β-galactosidase activities) for spacings smaller than 59.5 bp appeared to be anomalous (Figure 2, lower panel), e.g. low reporter expression (independent of IPTG induction) at 51.5 bp operator spacing. The data are also questionable because of the large-phase shift observed in the presence of IPTG inducer, an observation that is difficult to justify though physical models. Because of the close packing of the −35 promoter element and the upstream O_{sym} operator in these minimal constructs (Figure 1D), further control experiments were undertaken to clarify the roles of DNA sequence versus DNA looping in these results.

In cases where O_{sym} and the promoter −35 element are closely spaced, repressor binding to O_{sym} (and perhaps the O_{sym} sequence itself) has the potential to influence the function of the promoter −35 element. This issue was explored by creating a series of control constructs containing O_{sym} sequences but lacking O_2. Construct sequences are shown in the Supplementary Figure S2. DNA looping between operators cannot occur in these constructs. The results and interpretation are shown in Figure 3.

Figure 3A shows repression ratio (RR) data for O_{sym} at various positions upstream of −35, in the absence of O_2. The RR is the reporter expression in the presence of IPTG divided by the reporter expression in the absence of IPTG.

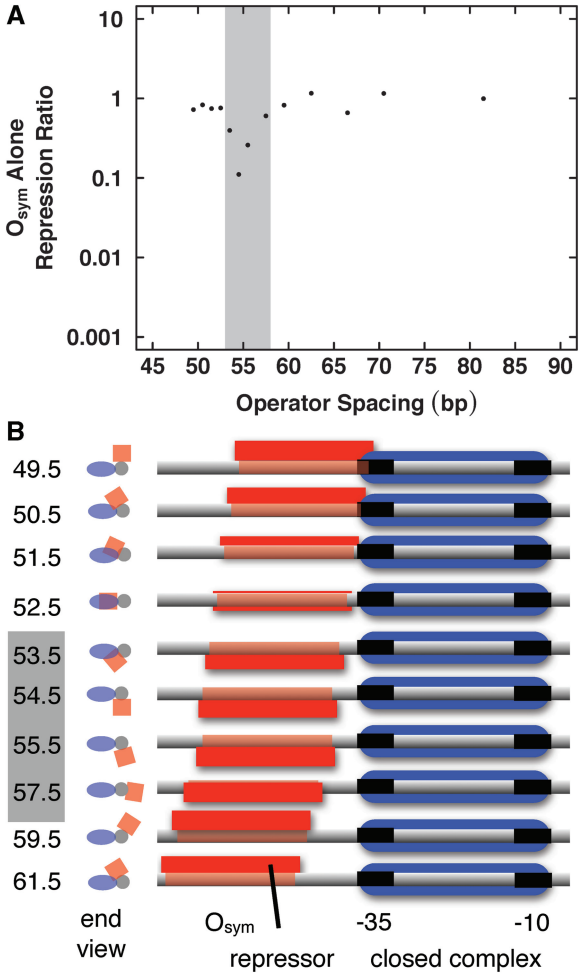

Figure 3. Evidence for loop-independent repression for O_{sym} near the promoter −35 element. (**A**) *In vivo* RR (+/− IPTG) for constructs with O_{sym} alone. (**B**) Schematic illustration of lac repressor (red rectangle) bound to O_{sym} operators just upstream of the test promoter. RNA polymerase in the closed complex projects into the page as shown schematically (blue oval). An end view (DNA observed from upstream) is displayed at left.

For constructs without any proximal operator, uniform repression rations of 1.0 are anticipated. This is observed for construct spacings as small as 59.5. However, constructs that place O_{sym} and −35 in closer proximity show evidence of loop-independent interference (Figure 3A). This suggests that lac repressor bound at O_{sym} directly interferes with the *lac* UV5 promoter. Interestingly, constructs with O_{sym} even closer to −35 (constructs 49.5–52.5, Figure 3B) show little loop-independent repression. In fact, the promoters in constructs 49.5 and 51.5 are weak even in the presence of IPTG inducer. We reasoned that face-of-the-helix considerations for repressor bound to O_{sym} and RNA polymerase bound to the −35 promoter element might be involved in these peculiar results. However, as shown in Figure 3B, the predicted helical disposition of the bound proteins does not provide a simple explanation. Based on a structural model for the helical face occupied by RNA polymerase in the closed complex (53), RNA polymerase

projects away from the viewer for the indicated constructs as shown in Figure 3B. The helical face occupied by lac repressor is also indicated schematically in Figure 3B. Constructs 53.5–57.5 show the greatest loop-independent repression in the absence of IPTG inducer (gray shading in Figure 3B), but these constructs are predicted to position lac repressor on the helical face 'away from' RNA polymerase where steric interference should be minimal. It is possible that the closest constructs appear not to cause repression because lac repressor can actually make 'favorable' contacts with RNA polymerase when repressor is positioned close to the −35 element and sharing the same helical face (55). Such contacts might be detected only for close spacings, and might be lost with helical dephasing for constructs 53.5–57.5. The phage λ repressor provides another precedent for such favorable RNA polymerase contacts with a repressor protein at close approach. Occupation of λ O_R3 operator by λ repressor stimulates the proximal P_{RM} promoter by cooperative protein–protein interactions (56). In any case, this analysis shows that the assumption of loop-dependent repression fails for constructs with operator spacings smaller than 59.5 in this promoter–operator configuration.

Analysis of repression loops from culled dataset

The experimental results described above suggest that data for DNA loops with operator spacings smaller than 59.5 should be excluded from the thermodynamic analysis because of loop-independent DNA sequence and/or repressor interference. Figure 4 shows that the 'culled' data set is fitted much better by the thermodynamic model of *lac* repression. The revised fitting parameters are shown in Table 1. The data pattern can be compared with a prior report (17). As discussed elsewhere (25), both Figures 2 and 4 confirm a ~5 bp discrepancy between RR peaks from the present work (55-, 66-, 77-bp operator separations) and those reported previously (59.5, 70.5, 81.5 and 92.5 bp) (17). The basis for this difference remains unclear, but one implication of the present work is that RR data (Figure 2, upper panel) can be misleading for short operator spacings. This may apply as well to the RR peak indicated at 59.5 bp in the prior study (17). Thus, RR data can be misinterpreted in quantitative DNA looping studies unless induced and uninduced reporter gene expression levels are independently examined in light of proper controls with disabled operators (Figure 3). In fact, our own formulation of the thermodynamic model used here was inspired by RR data that appeared to show multiple loop forms. Only when the raw expression data were analyzed did it become clear that the effect was due to different lac looping patterns in the absence and presence of IPTG inducer.

Effects of *E. coli* HU protein loss on minimal *lac* repression looping

Previous experiments have shown that *lac* repression looping is strongly disabled in *E. coli* strains lacking the sequence-non-specific architectural DNA bending protein HU (23–26). The minimum loop size examined

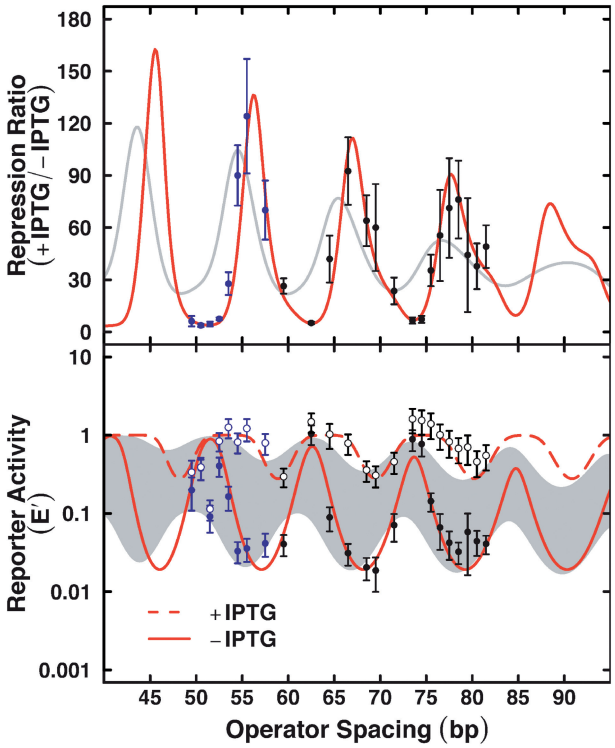

Figure 4. Reporter repression as a function of *lac* operator spacing for constructs studied here (transcription start site within downstream O_2). Data format is as in Figure 2 but limited to operator spacings >59 bp where repression is loop dependent. Excluded data points are shown in blue. Fitted parameters are shown in Table 1.

in previous experiments was 65 bp, with O_2 downstream of the UV5 promoter transcription start point. New data were collected in the ΔHU genetic background for the present constructs with operator spacings >59 bp. The results are shown in Figure 5, showing comparison with fits to the thermodynamic looping model from the earlier work (23), and parameters are reported in Table 1. Repression data in the absence of HU again show looping to be strongly disabled: repression for dephased operators in the absence of IPTG (peaks in E' data) is poor, comparable with repression in the presence of IPTG inducer. For ideally phased operators, repression is ~5-fold poorer than in the wild-type strain. Comparison of these fits in Table 1 shows that K°_{max}, the normalized equilibrium constant for formation of the optimum loop from a state with singly bound lac repressor, is reduced from 62 (wild-type) to 14 (ΔHU), while the apparent DNA twist constant increases >10%. Interestingly, the present constructs (transcription start site within O_2) appear more disabled with respect to overcoming DNA twist energy than the original constructs with transcription starting upstream of O_2 (black lines, Figure 5, bottom panel). The apparent DNA twist constant is >60% larger for the ΔHU mutation in the context of constructs with transcription initiation within O_2. As previously observed (23), there is little evidence of residual repression looping for the ΔHU strain in the presence of IPTG

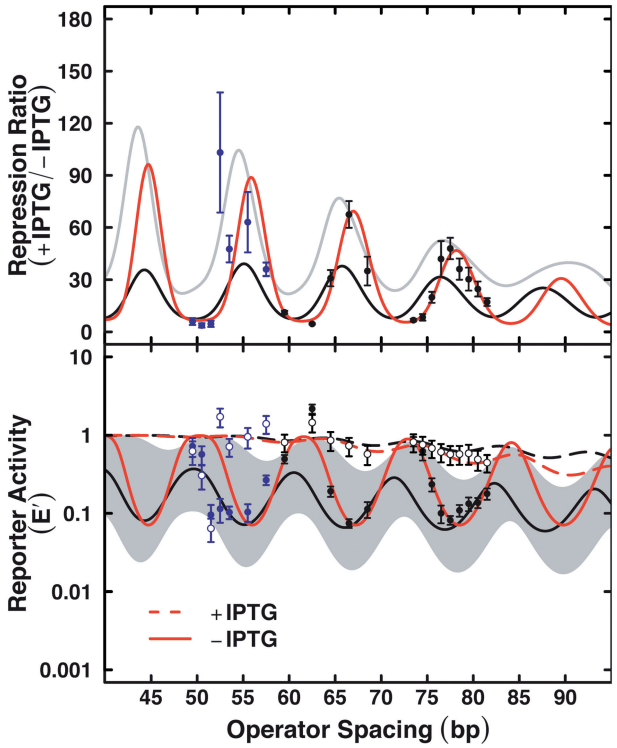

Figure 5. Reporter repression as a function of *lac* operator spacing for constructs studied here (transcription start site within downstream O_2) but in a ΔHU strain. Data format is as in Figure 2 and limited to operator spacings >59 bp where repression is loop dependent. Excluded data points are shown in blue. Previous data fits from Becker *et al.* (23) are shown by black lines, for comparison. Fitted parameters are shown in Table 1.

inducer. Reporter expression in the presence of IPTG increases slightly for shorter operator spacings (Figure 5).

Summary and implications

The present results indicate that DNA segments as short as approximately six helical turns can participate in effective repression loops with lac repressor protein *in vivo*. In contrast to what might be expected for DNA loops based on the WLC model, the repression pattern does not suggest increased resistance to bending or twisting with shorter loops. As previously observed (23), the amplitudes and extrema of E' oscillations with or without inducer are approximately constant over this range (Figure 4), even in the absence of the architectural nucleoid protein HU (Figure 5). This suggests that DNA twist inflexibility is the predominant obstacle to looping *in vivo*. Only for very weak looping in the presence of IPTG inducer and the absence of HU protein (Figure 5) is there *any* evidence for decreased repression with shorter loop lengths. Deletion of HU reduces the apparent looping equilibrium constant by almost 2-fold, while increasing the apparent DNA torsion constant by only 9%. These results again point to the involvement of nucleoid proteins in facilitating DNA repression looping (23–25).

These data do not reveal whether RNA polymerase is excluded from the repressed promoter held within a small loop. RNA polymerase may be sterically occluded from the promoter by crowding between two *lac* operators occupied by the repressor tetramer. It is also possible that the curvature of the constrained promoter, *per se*, inhibits RNA polymerase binding and initiation (57,58).

One goal of this work was to reconfigure the experimental promoter and downstream operator to allow the smallest possible spacings between operators while retaining an internal promoter. We show (Figure 2) that the results are potentially misleading without proper controls. Careful analysis of the repression when O_{sym} crowds the promoter −35 element shows loop-independent repression, and 'increased' expression suggests that repressor/polymerase interactions may be favorable at the closest spacings. Over the range of operator spacings where repression can be shown to be loop dependent (center-to-center spacings >59 bp), fits to the thermodynamic model show the effective DNA helical repeat to be near 11 bp/turn. The apparent DNA twist constant ($\sim 0.9 \times 10^{-19}$ erg cm) is 2- to 4-fold lower than observed for naked DNA *in vitro*. This discrepancy may reflect effects of repressor flexibility and nucleoid proteins, although deletion of HU does not substantially change the fitted value of the apparent twist constant.

Models

Most importantly, even for the shortest DNA loops that constrain an *E. coli* promoter *in vivo* (~40% of one persistence length), 'there is no evidence that DNA bending strain limits DNA looping'. This observation demonstrates a fundamental difference between the *in vivo* observation and expectations based on the WLC model *in vitro*. This puzzle might be solved by considering the possibility that lac repressor (LacI) is constraining a DNA loop 'within a negatively supercoiled plectoneme'. Figure 6 shows two models for LacI:DNA loops in superhelical DNA. Figure 6A shows LacI binding operators in plectonemic DNA. Negative supercoiling helps bring the operators into close contact, with crossovers consistent with the V-shaped repressor. Positions at which the repressor can make analogous contacts to an operator are separated by multiples of the helical repeat: to contact both repressor dimers in a V-shaped protein, the minor grooves of the two operators must be facing in roughly parallel directions. The model in Figure 6A would explain why the length dependence of DNA looping energy is small: loops of very different sizes make analogous contacts within the same DNA structure. The model also explains the apparent helical repeat of ~11 bp/turn: in plectonemic DNA, the apparent DNA helical repeat is larger than the DNA twist (54), because the patch on one dsDNA strand of the plectoneme that makes the closest approach to the other strand traces out a helical path on the surface of the DNA, so it requires more than one helical repeat to rotate around to an equivalent position relative to the other strand. As shown, the optimal spacing between operators is approximately half-integral because the DNA has traversed a ~180° bend through the apical loop of the supercoil (31), but if the twist changes within the apical loop the optimal spacing should also change.

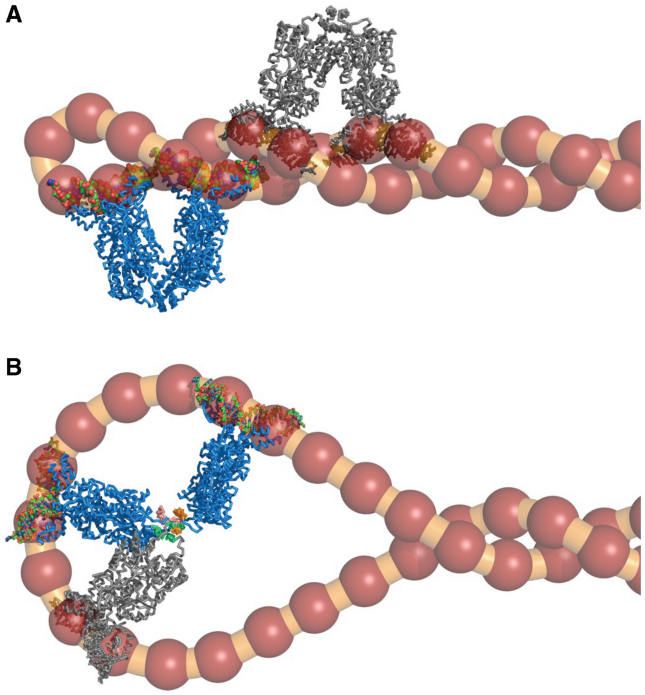

Figure 6. Schematic illustration of possible lac repression loops near the apex of a negatively supercoiled plectoneme. DNA is shown in gold with red markers every 10 bp. The LacI protein–operator complex in blue in part (**A**) is taken from the X-ray crystal structure [1lbg; (77)]. (**A**) Binding within the plectoneme. The DNA is modeled as a 500-bp minicircle with $\sigma = -0.18$ and the superhelical geometry parameters described in 'Materials and Methods' section. Operator separations in the two LacI:DNA loops shown correspond to ~5.5 turns (blue, left) or ~12.5 turns (gray, middle). (**B**) Binding within the apical loop. The DNA is modeled as a 500-bp minicircle with $\sigma = -0.06$, giving a radius for the circular part of the apical loop of ~90 Å. The blue protein illustrates one dimer of LacI rotated away from the other, anchored by the four-helix bundle tetramerization domain. The inter-dimer angle is ~100°, and the operators are approximately five helical turns apart. The gray protein illustrates the second dimer with an inter-dimer angle of ~160°, with the operators approximately eight helical turns apart.

Figure 6A resembles the antiparallel loops proposed by Adhya and coworkers (59) for loops anchored by GalR, modeled using rod mechanics for artificial hyperstable loops by Perkins and coworkers (60,61), and modeled with statistical mechanics and applied to repression data by Zhang *et al.* (31) as the 'LB' loop. We suggest that models like Figure 6A are reasonable for long separations between operators, but they cannot explain our data at short separations. To allow a ~60 bp LacI:DNA loop, the apical loop in the superhelix would need to be very small, requiring a superhelical density (approximately −0.2) that is much more negative than the average unrestrained value *in vivo* and for which there is no evidence.

Figure 6B illustrates LacI binding operators in the apical loop of superhelical DNA. A putative 'open form' of the repressor is shown, for which there is independent evidence (27,62,63). The blue protein illustrates one dimer of LacI rotated away from the other, anchored by the four-helix bundle tetramerization domain [as suggested by Steitz and coworkers (64)]. The inter-dimer angle is ~100°, and the operators are approximately five helical turns apart. The gray protein illustrates the second dimer with an inter-dimer angle of ~160°, with the operators approximately eight helical turns apart. The details of operator non-coplanarity are ignored here, but we suggest that the non-coplanarity makes even shorter loops impossible unless there are dramatic changes in the protein–DNA interface. DNA bending away from LacI is also ignored in this model. We propose that HU or other architectural proteins may enable bending of the intervening DNA to allow the needed translocation of the helix axis and also bending within the apical loop to accommodate the outward bending induced by the protein. The model in Figure 6B explains the lack of length dependence because, as in Figure 6A, different operator separations are accommodated within the same DNA geometry. The model does not provide an obvious rationalization for the change in helical repeat, but we suggest that twist strain in superhelical DNA may be concentrated in apical loops due to twist-bend coupling (65), or protein binding required for looping may require twist changes.

The model in Figure 6B was generated assuming a much more physiological σ (–0.06) than the model in Figure 6A. While the actual size of apical loops *in vivo* is unknown, using our simple geometric model and comparisons with more sophisticated theoretical treatments (66,67) and experimental electron microscopy (EM) and atomic force microscopy (AFM) images of plasmid DNA (68–70), we can assess a reasonable range of superhelical shapes and thus apical loop sizes over which the ideas in the figure may be applicable. First, in the limit of absorbing all of the superhelicity into a minimum-radius plectonemic superhelix, the negative writhe per helical turn of DNA in the plectoneme is much greater than physiological superhelical density. Thus, there is a significant amount of DNA 'left over' that partitions into branch junctions and apical loops, with the amount of remaining DNA being proportional to the assumed topological domain size. To provide a fair comparison to Figure 6A, Figure 6B assumes a 500-bp minicircle with a minimal superhelix radius, giving an apical loop radius of ~90 Å. For a 1000-bp domain, at $\sigma = -0.06$ the radius of the apical loop would be ~150 Å, and at $\sigma = -0.03$ ~180 Å. Under these conditions, there would be no steric barriers to forming shapes like those of Figure 6B, but on the other hand there would be less unstressed curvature in the apical loop and the observed insensitivity to DNA length and changes in apparent helical repeat might not be expected.

The assumed pitch and diameter of the superhelix dramatically affect the calculated size of apical loops. EM and AFM results as well as Monte Carlo simulations suggest that at physiological salt concentrations the diameter of apical loops is about the same or perhaps two to three times as large as the separation between the strands of the plectoneme, so that the DNA appears quite uniform nearly to the end of the apical loop (66–71). For a given superhelical density, we model this observation by adjusting the superhelix radius so that as much as possible of the DNA is contained in the plectoneme, with just enough DNA left over to form an arc closing the ends. Thus, in this limit of the 'loosest' possible supercoil, the radius

of the apical loop is minimized, becoming equal to the radius of the superhelix. The results are independent of assumed domain size, as observed in experiments on plasmids of different sizes (67,70). With these assumptions, at $\sigma = -0.06$ the radii of the superhelix and the apical loop are ~50 Å, and at $\sigma = -0.03$ ~100 Å, very similar to the apical loop size shown in Figure 6B.

In summary, the model of Figure 6A illustrates that very short loops are probably impossible at physiological superhelical density within a plectonemic helix. Figure 6B illustrates the idea that binding of different plausible LacI conformers within apical loops with a consistent geometry can explain the lack of operator spacing dependence for repression by short loops. Loops roughly the size shown in Figure 6 are seen experimentally and can form for a wide range of superhelical densities including the likely level of unrestrained supercoiling in the bacterial cell. Our proposal complements the previous calculations of Zhang *et al*. (31) showing that an open form of LacI would provide length-independent repression, but their model refers to a fixed open form of LacI that anchors different loop shapes as the operator spacing increases. Saiz and Vilar (72) have proposed multiple loop shapes to explain fine structure in our repression curves, but their models do not consider the effects of residual looping by inducer-bound LacI. RNA polymerase localization at apical loops was identified in 1992 (73), and more recently Travers and Muskhelishvili (74) have proposed that non-specific DNA binding proteins and transcription factors may act in part by controlling the formation of short plectonemic regions and thereby the availability of apical loops. Transient changes in superhelical density can control the binding of proteins that require (75) or permit (76) DNA untwisting.

This work illustrates that studies of small repression loops containing an *E. coli* promoter can be complicated by loop-independent repression at close promoter–operator spacings. *In vivo* testing of DNA strain in even smaller loops will require new designs where the promoter is positioned outside of the DNA loop.

SUPPLEMENTARY DATA

Supplementary data are available at NAR Online.

ACKNOWLEDGEMENTS

The authors acknowledge the excellent suggestions of the anonymous referees during the review of this manuscript.

FUNDING

Mayo Foundation; National Institutes of Health (grant GM075965 to L.J.M.); Summer Undergraduate Research Fellowship from Mayo Graduate School (to L.M.B., in part). Funding for open access charge: National Institutes of Health; Mayo Clinic.

Conflict of interest statement. None declared.

REFERENCES

1. Kratky,O. and Porod,G. (1949) Röntgenuntersuchung gelöster fadenmoleküle. *Recl. Trav. Chim. Pays-Bas*, **68**, 1106–1123.
2. Shimada,J. and Yamakawa,H. (1984) Ring-closure probabilities for twisted wormlike chains. Application to DNA. *Macromolecules*, **17**, 689–698.
3. Garcia,H.G., Grayson,P., Han,L., Inamdar,M., Kondev,J., Nelson,P.C., Phillips,R., Widom,J. and Wiggins,P.A. (2007) Biological consequences of tightly bent DNA: The other life of a macromolecular celebrity. *Biopolymers*, **85**, 115–130.
4. Widom,J. (2001) Role of DNA sequence in nucleosome stability and dynamics. *Q. Rev. Biophys.*, **34**, 269–324.
5. Virstedt,J., Berge,T., Henderson,R.M., Waring,M.J. and Travers,A.A. (2004) The influence of DNA stiffness upon nucleosome formation. *J. Struct. Biol.*, **148**, 66–85.
6. Tolstorukov,M.Y., Colasanti,A.V., McCandlish,D.M., Olson,W.K. and Zhurkin,V.B. (2007) A novel roll-and-slide mechanism of DNA folding in chromatin: implications for nucleosome positioning. *J. Mol. Biol.*, **371**, 725–738.
7. Rohs,R., West,S.M., Sosinsky,A., Liu,P., Mann,R.S. and Honig,B. (2009) The role of DNA shape in protein-DNA recognition. *Nature*, **461**, 1248–1253.
8. Caserta,M., Agricola,E., Churcher,M., Hiriart,E., Verdone,L., Di Mauro,E. and Travers,A. (2009) A translational signature for nucleosome positioning in vivo. *Nucleic Acids Res.*, **37**, 5309–5321.
9. Satchwell,S.C., Drew,H.R. and Travers,A.A. (1986) Sequence periodicities in chicken nucleosome core DNA. *J. Mol. Biol.*, **191**, 659–675.
10. Kaplan,N., Moore,I.K., Fondufe-Mittendorf,Y., Gossett,A.J., Tillo,D., Field,Y., LeProust,E.M., Hughes,T.R., Lieb,J.D., Widom,J. *et al*. (2009) The DNA-encoded nucleosome organization of a eukaryotic genome. *Nature*, **458**, 362–366.
11. Laurens,N., Bellamy,S.R., Harms,A.F., Kovacheva,Y.S., Halford,S.E. and Wuite,G.J. (2009) Dissecting protein-induced DNA looping dynamics in real time. *Nucleic Acids Res.*, **37**, 5454–5464.
12. Paull,T.T., Haykinson,M.J. and Johnson,R.C. (1993) The nonspecific DNA-binding and -bending proteins HMG1 and HMG2 promote the assembly of complex nucleoprotein structures. *Genes Dev.*, **7**, 1521–1534.
13. Paull,T.T., Haykinson,M.J. and Johnson,R.C. (1994) HU and functional analogs in eukaryotes promote Hin invertasome assembly. *Biochimie*, **76**, 992–1004.
14. Wedel,A., Weiss,D.S., Popham,D., Droge,P. and Kustu,S. (1990) A bacterial enhancer functions to tether a transcriptional activator near a promoter. *Science*, **248**, 486–490.
15. Harmer,T., Wu,M. and Schleif,R. (2001) The role of rigidity in DNA looping-unlooping by AraC. *Proc. Natl Acad. Sci. USA*, **98**, 427–431.
16. Mossing,M.C. and Record,M.T. Jr (1986) Upstream operators enhance repression of the *lac* promoter. *Science*, **233**, 889–892.
17. Muller,J., Oehler,S. and Müller-Hill,B. (1996) Repression of lac promoter as a function of distance, phase and quality of an auxiliary lac operator. *J. Mol. Biol.*, **257**, 21–29.
18. Oehler,S. and Müller-Hill,B. (2009) High local concentration: a fundamental strategy of life. *J. Mol. Biol.*, **395**, 242–253.
19. Dobi,K.C. and Winston,F. (2007) Analysis of transcriptional activation at a distance in Saccharomyces cerevisiae. *Mol. Cell. Biol.*, **27**, 5575–5586.
20. Bellomy,G., Mossing,M. and Record,M. (1988) Physical properties of DNA *in vivo* as probed by the length dependence of the *lac* operator looping process. *Biochemistry*, **27**, 3900–3906.
21. Law,S.M., Bellomy,G.R., Schlax,P.J. and Record,M.T. Jr (1993) In vivo thermodynamic analysis of repression with and without looping in lac constructs. Estimates of free and local lac repressor concentrations and of physical properties of a region of supercoiled plasmid DNA in vivo. *J. Mol. Biol.*, **230**, 161–173.
22. Oehler,S., Eismann,E.R., Kramer,H. and Müller-Hill,B. (1990) The three operators of the lac operon cooperate in repression. *EMBO J.*, **9**, 973–979.
23. Becker,N.A., Kahn,J.D. and Maher,L.J. 3rd (2005) Bacterial repression loops require enhanced DNA flexibility. *J. Mol. Biol.*, **349**, 716–730.

24. Becker,N.A., Kahn,J.D. and Maher,L.J. 3rd (2007) Effects of nucleoid proteins on DNA repression loop formation in *Escherichia coli*. *Nucleic Acids Res.*, **35**, 3988–4000.
25. Becker,N.A., Kahn,J.D. and Maher,L.J. 3rd (2008) Eukaryotic HMGB proteins as replacements for HU in *E. coli* repression loop formation. *Nucleic Acids Res.*, **36**, 4009–4021.
26. Sebastian,N.T., Bystry,E.M., Becker,N.A. and Maher,L.J. 3rd (2009) Enhancement of DNA flexibility in vitro and in vivo by HMGB box A proteins carrying box B residues. *Biochemistry*, **48**, 2125–2134.
27. Wong,O.K., Guthold,M., Erie,D.A. and Gelles,J. (2008) Interconvertible lac repressor-DNA loops revealed by single-molecule experiments. *PLoS Biol.*, **6**, e232.
28. Han,L., Garcia,H.G., Blumberg,S., Towles,K.B., Beausang,J.F., Nelson,P.C. and Phillips,R. (2009) Concentration and length dependence of DNA looping in transcriptional regulation. *PLoS ONE*, **4**, e5621.
29. Bintu,L., Buchler,N.E., Garcia,H.G., Gerland,U., Hwa,T., Kondev,J. and Phillips,R. (2005) Transcriptional regulation by the numbers: models. *Curr. Opin. Genet. Dev.*, **15**, 116–124.
30. Zhang,Y., McEwen,A.E., Crothers,D.M. and Levene,S.D. (2006) Statistical-mechanical theory of DNA looping. *Biophys. J.*, **90**, 1903–1912.
31. Zhang,Y., McEwen,A.E., Crothers,D.M. and Levene,S.D. (2006) Analysis of in-vivo LacR-mediated gene repression based on the mechanics of DNA looping. *PLoS ONE*, **1**, e136.
32. Swigon,D., Coleman,B.D. and Olson,W.K. (2006) Modeling the Lac repressor-operator assembly: the influence of DNA looping on Lac repressor conformation. *Proc. Natl Acad. Sci. USA*, **103**, 9879–9884.
33. Balaeff,A., Mahadevan,L. and Schulten,K. (2004) Structural basis for cooperative DNA binding by CAP and lac repressor. *Structure*, **12**, 123–132.
34. Villa,E., Balaeff,A. and Schulten,K. (2005) Structural dynamics of the lac repressor-DNA complex revealed by a multiscale simulation. *Proc. Natl Acad. Sci. USA*, **102**, 6783–6788.
35. Ringrose,L., Chabanis,S., Angrand,P.O., Woodroofe,C. and Stewart,A.F. (1999) Quantitative comparison of DNA looping in vitro and in vivo: chromatin increases effective DNA flexibility at short distances. *EMBO J.*, **18**, 6630–6641.
36. Travers,A., Ner,S. and Churchill,M. (1994) DNA chaperones: A solution to a persistence problem. *Cell*, **77**, 167–169.
37. Aki,T. and Adhya,S. (1997) Repressor induced site-specific binding of HU for transcriptional regulation. *EMBO J.*, **16**, 3666–3674.
38. Lewis,D.E. and Adhya,S. (2002) In vitro repression of the gal promoters by GalR and HU depends on the proper helical phasing of the two operators. *J. Biol. Chem.*, **277**, 2498–2504.
39. Lia,G., Bensimon,D., Croquette,V., Allemand,J.F., Dunlap,D., Lewis,D.E., Adhya,S. and Finzi,L. (2003) Supercoiling and denaturation in Gal repressor/heat unstable nucleoid protein (HU)-mediated DNA looping. *Proc. Natl Acad. Sci. USA*, **100**, 11373–11377.
40. Paull,T. and Johnson,R. (1995) DNA looping by Saccharomyces cerevisiae high mobility group proteins NHP6A/B. *J. Biol. Chem.*, **270**, 8744–8754.
41. Cloutier,T.E. and Widom,J. (2004) Spontaneous sharp bending of double-stranded DNA. *Mol. Cell*, **14**, 355–362.
42. Cloutier,T.E. and Widom,J. (2005) DNA twisting flexibility and the formation of sharply looped protein-DNA complexes. *Proc. Natl Acad. Sci. USA*, **102**, 3645–3650.
43. Wiggins,P.A., Van Der Heijden,T., Moreno-Herrero,F., Spakowitz,A., Phillips,R., Widom,J., Dekker,C. and Nelson,P.C. (2006) High flexibility of DNA on short length scales probed by atomic force microscopy. *Nat. Nanotechnol.*, **1**, 137–141.
44. Lankas,F., Lavery,R. and Maddocks,J.H. (2006) Kinking occurs during molecular dynamics simulations of small DNA minicircles. *Structure*, **14**, 1527–1534.
45. Du,Q., Kotlyar,A. and Vologodskii,A. (2008) Kinking the double helix by bending deformation. *Nucleic Acids Res.*, **36**, 1120–1128.
46. Du,Q., Smith,C., Shiffeldrim,N., Vologodskaia,M. and Vologodskii,A. (2005) Cyclization of short DNA fragments and bending fluctuations of the double helix. *Proc. Natl Acad. Sci. USA*, **102**, 5397–5402.
47. Mastroianni,A.J., Sivak,D.A., Geissler,P.L. and Alivisatos,A.P. (2009) Probing the conformational distributions of subpersistence length DNA. *Biophys. J.*, **97**, 1408–1417.
48. Mathew-Fenn,R.S., Das,R. and Harbury,P.A. (2008) Remeasuring the double helix. *Science*, **322**, 446–449.
49. McCauley,M., Hardwidge,P.R., Maher,L.J. 3rd and Williams,M.C. (2005) Dual binding modes for an HMG domain from human HMGB2 on DNA. *Biophys. J.*, **89**, 353–364.
50. Hochschild,A. and Ptashne,M. (1986) Cooperative binding of lambda repressors to sites separated by integral turns of the DNA helix. *Cell*, **44**, 681–687.
51. Whipple,F.W. (1998) Genetic analysis of prokaryotic and eukaryotic DNA-binding proteins in *Escherichia coli*. *Nucleic Acids Res.*, **26**, 3700–3706.
52. Boles,T.C., White,J.H. and Cozzarelli,N.R. (1990) Structure of plectonemically supercoiled DNA. *J. Mol. Biol.*, **213**, 931–951.
53. Murakami,K.S., Masuda,S., Campbell,E.A., Muzzin,O. and Darst,S.A. (2002) Structural basis of transcription initiation: an RNA polymerase holoenzyme-DNA complex. *Science*, **296**, 1285–1290.
54. Bloomfield,V.A., Crothers,D.M. and Tinoco,I. (2000) *Nucleic Acids: Structures, Properties and Functions*. University Science Press, Mill Valley, CA.
55. Straney,S.B. and Crothers,D.M. (1987) Lac repressor is a transient gene-activating protein. *Cell*, **51**, 699–707.
56. Ptashne,M., Backman,K., Humayun,M.Z., Jeffrey,A., Maurer,R., Meyer,B. and Sauer,R.T. (1976) Autoregulation and function of a repressor in bacteriophage lambda. *Science*, **194**, 156–161.
57. Choy,H.E., Park,S.-W., Parrack,P. and Adhya,S. (1995) Transcription regulation by inflexibility of promoter DNA in a looped complex. *Proc. Natl Acad. Sci. USA*, **92**, 7327–7331.
58. Lionberger,T. and Meyhofer,E. (2010) Highly bent DNA: A novel repressor of T7 RNA polymerase. *Biophys. J.*, **98**, 69a.
59. Semsey,S., Virnik,K. and Adhya,S. (2005) A gamut of loops: meandering DNA. *Trends Biochem. Sci.*, **30**, 334–341.
60. Goyal,S., Lillian,T., Blumberg,S., Meiners,J.C., Meyhofer,E. and Perkins,N.C. (2007) Intrinsic curvature of DNA influences LacR-mediated looping. *Biophys. J.*, **93**, 4342–4359.
61. Lillian,T.D., Goyal,S., Kahn,J.D., Meyhofer,E. and Perkins,N.C. (2008) Computational analysis of looping of a large family of highly bent DNA by LacI. *Biophys. J.*, **95**, 5832–5842.
62. Edelman,L.M., Cheong,R. and Kahn,J.D. (2003) Fluorescence resonance energy transfer over approximately 130 basepairs in hyperstable lac repressor-DNA loops. *Biophys. J.*, **84**, 1131–1145.
63. Kahn,J.D., Cheong,R., Mehta,R.A., Edelman,L.M. and Morgan,M.A. (2006) Flexibility and control of DNA loops. *Biophys. Rev. Lett.*, **1**, 327–341.
64. Friedman,A.M., Fischmann,T.O. and Steitz,T.A. (1995) Crystal structure of lac repressor core tetramer and its implications for DNA looping. *Science*, **268**, 1721–1727.
65. Marko,J.F. and Siggia,E.D. (1994) Fluctuations and supercoiling of DNA. *Science*, **265**, 506–508.
66. Schlick,T. (1995) Modeling superhelical DNA: recent analytical and dynamic approaches. *Curr. Opin. Struct. Biol.*, **5**, 245–262.
67. Vologodskii,A. and Cozzarelli,N.R. (1996) Effect of supercoiling on the juxtaposition and relative orientation of DNA sites. *Biophys. J.*, **70**, 2548–2556.
68. Cherny,D.I. and Jovin,T.M. (2001) Electron and scanning force microscopy studies of alterations in supercoiled DNA tertiary structure. *J. Mol. Biol.*, **313**, 295–307.
69. Lyubchenko,Y.L. and Shlyakhtenko,L.S. (1997) Visualization of supercoiled DNA with atomic force microscopy *in situ*. *Proc. Natl Acad. Sci. USA*, **94**, 496–501.
70. Boles,T.C., White,J.H. and Cozzarelli,N.R. (1990) Structure of plectonemically supercoiled DNA. *J. Mol. Biol.*, **213**, 931–951.
71. Bednar,J., Furrer,P., Stasiak,A., Dubochet,J., Egelman,E.H. and Bates,A.D. (1994) The twist, writhe, and overall shape of supercoiled DNA change during counterion-induced transition from a loosely to a tightly interwound superhelix: possible implications for DNA structure *in vivo*. *J. Mol. Biol.*, **235**, 825–847.
72. Saiz,L. and Vilar,J.M. (2007) Multilevel deconstruction of the in vivo behavior of looped DNA-protein complexes. *PLoS ONE*, **2**, e355.

73. ten Heggeler-Bordier,B., Wahli,W., Adrian,M., Stasiak,A. and Dubochet,J. (1992) The apical localization of transcribing RNA polymerases on supercoiled DNA prevents their rotation around the template. *EMBO J.*, **11**, 667–672.
74. Travers,A. and Muskhelishvili,G. (2007) A common topology for bacterial and eukaryotic transcription initiation? *EMBO Rep.*, **8**, 147–151.
75. Kouzine,F., Sanford,S., Elisha-Feil,Z. and Levens,D. (2008) The functional response of upstream DNA to dynamic supercoiling in vivo. *Nat. Struct. Mol. Biol.*, **15**, 146–154.
76. Kahn,J.D. (2000) Topological effects of the TATA box binding protein on minicircle DNA and a possible thermodynamic linkage to chromatin remodeling. *Biochemistry*, **39**, 3520–3524.
77. Lewis,M., Chang,G., Horton,N.C., Kercher,M.A., Pace,H.C., Schumacher,M.A., Brennan,R.G. and Lu,P. (1996) Crystal structure of the lactose operon repressor and its complexes with DNA and inducer. *Science*, **271**, 1247–1254.